

# Polymer-Polymer Mutual Diffusion Using Transmission FTIR Spectroscopy

Martin S. High,\*† Paul C. Painter, and Michael M. Coleman\*

Department of Materials Science and Engineering, The Pennsylvania State University, University Park, Pennsylvania 16802

Received July 29, 1991; Revised Manuscript Received October 16, 1991

**ABSTRACT:** A unique method has been developed to experimentally observe mutual diffusion of poly(ethylene-co-methacrylic acid) (EMAA) and poly(vinyl methyl ether) (PVME) using conventional transmission FTIR spectroscopy. Using closed boundary conditions and assuming a composition-independent diffusion coefficient, a value of  $D = 6.5 \times 10^{-16} \text{ cm}^2/\text{s}$  was determined at 110 °C.

## Introduction

Previous polymer diffusion measurements have emphasized the determination of self-diffusion coefficients either in pure polymers or in mixtures with solvents or other polymers. These measurements are usually performed using radioactive tracers,<sup>1-3</sup> NMR pulsed-field gradient techniques,<sup>4-6</sup> or forward recoil spectroscopy (FRS).<sup>7</sup> To a much lesser degree, mutual diffusion or interdiffusion coefficients have been studied using radioactive tracers,<sup>8</sup> FRS,<sup>9</sup> SEM X-ray fluorescence,<sup>10-12</sup> and SAX.<sup>13</sup> To a limited extent, infrared spectroscopy has also been employed to observe diffusion in polymer blends via a "microdensitometry" technique using deuterium-labeled polymers.<sup>14-17</sup> In this paper we describe a unique method of observing polymer-polymer diffusion in a miscible binary system where there are hydrogen-bonding functional groups using standard transmission FTIR spectroscopy.

Infrared spectroscopy is widely recognized as the preeminent probe for studying hydrogen bonding in both low and high molecular weight materials and their mixtures. During the course of the past 5 years we have developed a theoretical model to describe the thermodynamics of binary polymer mixtures containing strong directionally specific interactions, especially hydrogen bonds.<sup>18</sup> Computer programs have been developed to calculate the fraction of interacting groups, the free energy of mixing, phase diagrams, miscibility windows, and maps.<sup>18</sup> It is this facility for being able to quantitatively determine the number of interacting groups in specific miscible polymer blends and relate these measurements to theoretical values based upon the stoichiometry of the system that allows us to employ transmission infrared spectroscopy to directly measure mutual diffusion.

## Experimental Section

The two polymers that form the diffusion couple described in this paper are a poly(ethylene-co-methacrylic acid) containing 26 wt % methacrylic acid (EMAA [26]) and poly(vinyl methyl ether) (PVME). The EMAA[26] copolymer, which has been described previously,<sup>19</sup> was obtained from E. I. du Pont de Nemours & Co. EMAA[26] contains enough methacrylic acid to preclude crystallinity from the ethylene portion of the copolymer but still has a relatively low glass transition temperature (~50 °C). The PVME was obtained from Polysciences, Inc. It is an amorphous polymer with a  $T_g$  of -27 °C and a reported molecular weight ( $M_w = 62\,700$ ,  $M_n = 35\,900$ ). Both polymers were used as received without further purification.

\* To whom correspondence should be addressed.

† Current address: School of Chemical Engineering, Oklahoma State University, Stillwater, OK 74078.

Polymer films of pure EMAA[26] and pure poly(vinyl methyl ether) (PVME) were cast from a 1% solution in tetrahydrofuran (THF) onto separate KBr windows. The majority of the THF immediately evaporated from the polymer film, and the remaining THF was removed by placing the sample in a vacuum desiccator at room temperature for at least 24 h. The two polymer films were then placed in contact as depicted in the schematic shown in Figure 1.

This KBr-EMAA-PVME-KBr "sandwich", together with an aluminum foil beam limiter (included for reasons discussed later), was placed in a demountable cell and introduced into an FTIR spectrometer. The diffusion couple was analyzed via transmission FTIR spectroscopy at room temperature, and this measurement represents the initial condition. The sample was then removed and placed in a mechanical convection oven at 110 °C. At regular intervals, the diffusion couple was removed from the oven and an FTIR analysis performed to monitor the diffusion of the two polymers. During the early stages of mixing spectra were recorded at approximately every 3-6 h.

In order to determine diffusion coefficients from the infrared diffusion data, we need to know at least the thickness of the EMAA[26] polymer film. A calibration curve of the absolute absorbance (area) of the characteristic IR band at ~1700  $\text{cm}^{-1}$  as a function of the mass of EMAA[26] polymer in the IR beam was prepared and is shown in Figure 2. Quantitative amounts of the polymer were cast from a solution of known concentration onto a KBr window and completely contained within the IR beam. For the diffusion samples, an aluminum foil beam limiter with a 7-mm hole is used to determine the thickness of the sample. Employing the calibration curve, the mass of EMAA[26] in the area exposed to the IR beam with the beam limiter in place is given by the area under the 1700- $\text{cm}^{-1}$  band. Given a density of EMAA[26], the thickness of the EMAA[26] film (0.187  $\mu\text{m}$ ) can be readily calculated.

All of the FTIR analysis described in this paper was performed on a Digilab FTS-60 spectrometer using 64 averaged scans at a resolution of 2  $\text{cm}^{-1}$ .

## FTIR and the Thermodynamics of Hydrogen Bonding

We have previously studied EMAA blends with a variety of polyethers,<sup>19,20</sup> poly(vinylpyridines),<sup>21</sup> and polyoxazolines.<sup>22</sup> FTIR was employed as the primary characterization tool, and one example, shown in Figure 3, should suffice to illustrate the relative ease of measurement of the fraction of carboxylic acid groups that are hydrogen bonded to ether groups in a miscible EMAA-poly(vinyl methyl ether) (PVME) blend.<sup>20</sup> The infrared band at ~1700  $\text{cm}^{-1}$  is assigned to the carboxylic acid dimer (self-association), while the band at ~1730  $\text{cm}^{-1}$  is attributed to "free" carbonyl groups in those species where there is a carboxylic acid-ether interaction (Scheme I). Thus the fraction of carboxylic acid moieties involved in interactions with ether groups may be calculated from a measurement

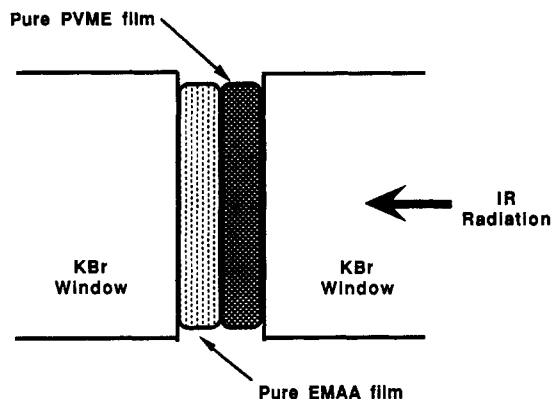


Figure 1. Schematic of the experimental technique used for observing mutual diffusion for the EMAA[26]-PVME couple.

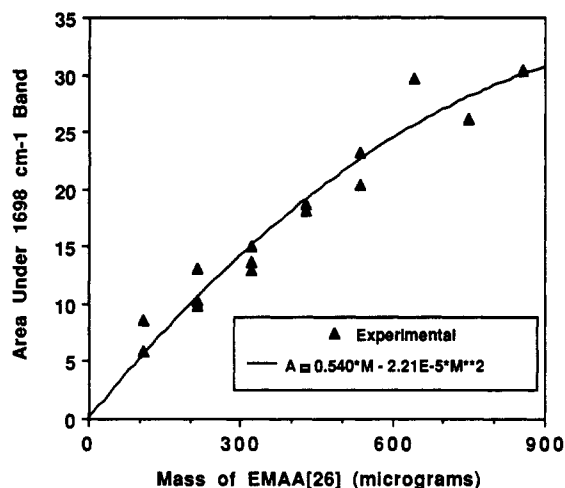


Figure 2. Mass calibration curve for EMAA[26] based on the area under the 1698-cm<sup>-1</sup> band.

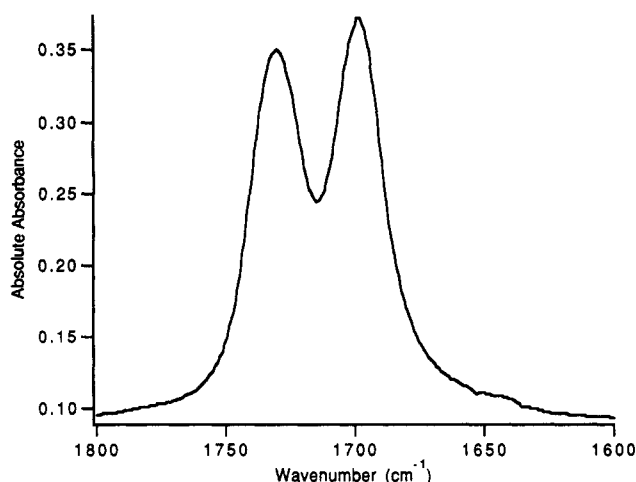


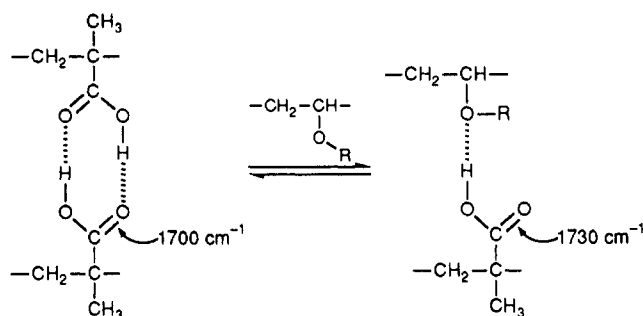
Figure 3. Spectrum recorded at room temperature in the carbonyl stretching region of a 50:50 wt % blend of EMAA[26] and PVME.

of the relative areas of bands in the spectra of blends of varying composition and at different temperatures, given that one has previously determined the ratio of the absorption coefficients for these two bands.<sup>18</sup>

The relationship between FTIR observations of the stoichiometry of hydrogen bonding and the thermodynamics of EMAA-PVME blends has been previously described using an association model.<sup>18,19</sup> Self-association of carboxylic acid groups in EMAA is given by the equilibrium scheme



#### Scheme I



Similarly, interassociation between the acid groups in EMAA and the ether oxygens in PVME is given by



Equilibrium constants,  $K_B$  and  $K_A$ , are defined in terms of volume fractions and are based upon a standard treatment of competing chemical equilibria. Accordingly, the volume fractions of dimerized and free carboxylic acid groups were shown to be given by the solution of the following set of equations:<sup>18,20</sup>

$$K_B = \frac{\Phi_{B_2}}{\Phi_{B_1}^2} \quad (3)$$

$$K_A = \frac{\Phi_{BA}}{\Phi_{A_1} \Phi_{B_1}} \left[ \frac{r}{1+r} \right] \quad (4)$$

$$\Phi_B = \Phi_{B_1} \left[ 1 + \frac{K_A \Phi_{A_1}}{r} \right] + 2K_B \Phi_{B_1}^2 \quad (5)$$

$$\Phi_A = \Phi_{A_1} [1 + K_A \Phi_{B_1}] \quad (6)$$

where  $\Phi_{B_1}$ ,  $\Phi_{B_2}$ ,  $\Phi_{A_1}$ , and  $\Phi_{BA}$  are the volume fractions of the carboxylic acid monomers, carboxylic acid dimers, unassociated ethers, and associated carboxylic acid-ether groups, respectively. The parameter  $r$  is the ratio of the molar volumes of the polymer repeat units,  $V_A/V_B$ . The volume fractions of the non-self-associating species A and self-associating species B are denoted as  $\Phi_A$  and  $\Phi_B$ .

We have previously described in detail the relationship between the equilibrium constants and the experimentally determined fraction of free carbonyl bands in EMAA-polyether blends and have shown how such information can be related to the phase diagrams of such systems.<sup>18,20</sup> In studying the diffusion of an EMAA-polyether couple, the driving force is the chemical potential gradient of both species, as dictated by Fick's law. To avoid complications from possible phase separation, we require a completely miscible system at the experimental temperature of interest. Calculations performed in the manner described previously indicate that PVME is miscible at ambient temperature, with EMAA copolymers containing up to approximately 98 wt % methacrylic acid.<sup>18</sup> In addition, the calculated phase diagram of the EMAA[26]-PVME couple predicts a single phase over the entire accessible temperature range (0–200 °C).

#### Polymer-Polymer Diffusion Measurements Using FTIR

If a pure film of EMAA[26] is placed in contact with a pure film of PVME, then the materials will slowly diffuse and ultimately achieve phase equilibrium corresponding

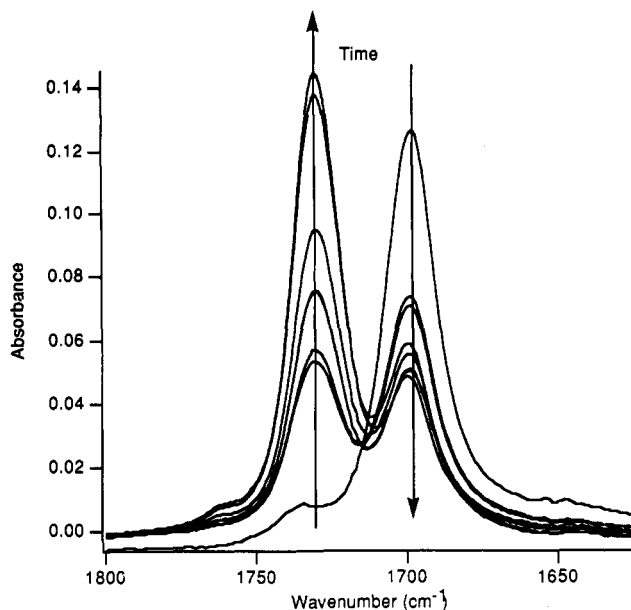


Figure 4. FTIR spectra of the EMAA[26]-PVME diffusion couple as a function of time at 110 °C.

to a single homogeneous phase. In our experimental methodology the observation of polymer-polymer diffusion in the EMAA[26]-PVME diffusion couple rests upon the detection of the specific interaction that occurs between the two polymers (i.e., the "free" carbonyl group formed upon interaction between the carboxylic acid-ether groups; Scheme I).

Typical FTIR spectra recorded as a function of time at 110 °C are shown in Figure 4. Initially, at  $t = 0$ , the EMAA[26] and PVME have not diffused to any extent and the spectrum is identical to that of pure EMAA[26]. To reiterate, the dominant band at  $\sim 1700\text{ cm}^{-1}$  corresponds to the large fraction of carboxylic acid dimers present in the essentially pure EMAA copolymer, and there is no significant contribution detected at  $\sim 1730\text{ cm}^{-1}$  arising from acid-ether interactions. (The weak shoulder present at  $\sim 1735\text{ cm}^{-1}$  at  $t = 0$  is not due to diffusion but to a minor amount of ester groups present in the EMAA copolymer.<sup>19</sup> This is taken into account and does not significantly affect our measurements or interpretation.) With increasing time the EMAA[26] and PVME begin to diffuse together and the infrared band at  $1730\text{ cm}^{-1}$  increases at the expense of the  $1700\text{-cm}^{-1}$  band. In other words, we are observing the mutual diffusion of EMAA[26] and PVME by the increase in acid-ether interactions and the simultaneous reduction of the number of carboxylic acid dimers.

A quantitative measure of the fraction of free EMAA[26] carbonyl groups (which is equivalent to the fraction of EMAA carboxylic acid groups involved in acid-ether interactions) may be calculated from

$$f_F = \frac{A_F}{A_F + A_D/ar} \quad (7)$$

where  $A_F$  is the area under the band at  $1728\text{ cm}^{-1}$ ,  $A_D$  is the area under the band at  $1730\text{ cm}^{-1}$ , and  $ar$  is the ratio of the absorption coefficients of the two bands ( $a_D/a_F$ ) which was previously determined to be 1.6.<sup>20</sup> The results of curve fitting this region of the spectrum are listed in Table I.

### Mathematical Analysis of the Diffusion Process

The analysis of the experimental data presented in Table I requires a mathematical connection between the fraction

Table I  
Experimental Peak Areas for the Carbonyl Region of  
EMAA[26] and the Resulting Fraction of Free Carbonyls

time, h	area		fraction of free carbonyls
	1698 $\text{cm}^{-1}$	1730 $\text{cm}^{-1}$	
0.0	3.778	0	0.00
8.9	2.318	1.022	0.41
14.3	2.188	1.089	0.44
24.0	1.458	1.681	0.65
31.0	1.396	1.669	0.66
48.5	1.406	2.202	0.71
72.7	1.293	3.235	0.80
313.8	0.996	3.456	0.85

of free carbonyls, the composition, and, ultimately, the diffusion coefficient of this system. We will first consider the relationship between the fraction of free carbonyls and the concentration of species and then later incorporate the relationship between the composition and the diffusion coefficient.

The fraction of free carbonyl groups is a function of the composition of the system. Since the two components are diffusing together, the overall composition of the system is a function of distance along the diffusion path,  $z$ , and the time,  $t$ . Since the IR measurement is performed in transmission, parallel to the diffusion path, the infrared beam is sampling the entire diffusion path at any given time. Mathematically, this is equivalent to an integral along the diffusion path and this is the quantity that we need to relate to experimental observations. If we chose a very thin slice of material perpendicular to the diffusion path and the IR beam with a thickness  $dz$ , the contribution to the IR band at  $1700\text{ cm}^{-1}$  for the dimerized carboxylic acid groups within that slice,  $dA_D$ , is proportional to the familiar product of absorption coefficient, concentration, and the path length:

$$dA_D(z,t) = a_D \Phi_D(z,t) dz \quad (8)$$

where  $\Phi_D(z,t)$  is the volume fraction of carboxylic acid dimers within the slice. Equations of this type are usually written in terms of molar concentration, but the conversion to volume fraction involves a simple constant that can be incorporated into the absorption coefficient and factors out in subsequent expressions. In a similar manner, the contribution to the overall absorption band for the free carbonyl groups within the slice,  $dA_F$ , is given by

$$dA_F(z,t) = a_F \Phi_F(z,t) dz \quad (9)$$

where  $\Phi_F(z,t)$  is the concentration of free carbonyls within the slice. Since we are interested in comparing the total IR absorption through the complete diffusion length, eqs 8 and 9 must be integrated over the thickness of the EMAA[26] and PVME films:

$$A_D(t) = \int_{-L_B}^{L_A} dA_D(z,t) = \int_{-L_B}^{L_A} a_D \Phi_D(z,t) dz \quad (10)$$

$$A_F(t) = \int_{-L_B}^{L_A} dA_F(z,t) = \int_{-L_B}^{L_A} a_F \Phi_F(z,t) dz \quad (11)$$

where  $L_B$  and  $L_A$  are the thicknesses of EMAA[26] and PVME, respectively.  $A_D(t)$  and  $A_F(t)$  can then be used to calculate the fraction of free carbonyl groups as a function of time.

The next step in the analysis is to calculate the volume fraction of carboxylic acid dimers,  $\Phi_D(z,t)$ , and free carbonyl groups,  $\Phi_F(z,t)$ , as a function of distance and time. Assume for the moment the volume fraction of the EMAA[26] as a function of distance and time,  $\Phi(z,t)$ , is known. The actual calculation of this quantity will come from the diffusion equations discussed later. Equations

5 and 6 can be combined to form a cubic equation in  $\Phi_{B_1}$  which can be solved analytically for the volume fraction of monomeric carboxylic acid groups which can then be used in conjunction with eqs 3 and 4 to calculate the volume fractions of  $\Phi_{B_2}$  ( $\equiv \Phi_D$ ) and  $\Phi_{AB}$  ( $\equiv \Phi_F$ ).  $K_A$  and  $K_B$  have been determined previously and are approximately  $10^2$  and  $4 \times 10^4$ , respectively.

The fraction free as a function of time,  $f_F(t)$ , is then calculated from eqs 7, 10, and 11:

$$f_F(t) = \frac{\int_{-L_B}^{L_A} \Phi_{AB}(z,t) dz}{\int_{-L_B}^{L_A} \Phi_{AB}(z,t) dz + \frac{1}{aF} \int_{-L_B}^{L_A} \Phi_{B_2}(z,t) dz} \quad (12)$$

Implicit in this calculation is the assumption that the hydrogen bonds formed during the diffusion process are in local equilibrium. Since the rates of formation and breaking hydrogen bonds are many orders of magnitude greater than the diffusion process, this is a valid approximation.

Equation 12 represents a computational scheme to calculate the fraction of free carbonyl groups given the concentration profile of the diffusion couple at any given time. This concentration profile is derived from the species continuity equation. The species continuity equation in one dimension is given by<sup>23</sup>

$$\frac{\partial \rho_B}{\partial t} + \frac{\partial(\rho_B \bar{v})}{\partial z} - \frac{\partial}{\partial z} \left[ D(\rho_B) \frac{\partial \rho_B}{\partial z} \right] = 0 \quad (13)$$

where  $\rho_B$  is the mass density of the EMAA[26] copolymer,  $\bar{v}$  is the velocity relative to the volume average velocity, and  $D$  is the mutual diffusion coefficient which is generally dependent upon composition. This is a result of the combination of material balances taking into account the contributions to convection and diffusion and describes the molecular diffusion relative to the volume average velocity of the system. The contributions from convection are zero if there is no volume change on mixing. In this case, the volume average velocity,  $\bar{v}$ , of the system vanishes. The species continuity equation then becomes

$$\frac{\partial \rho_B}{\partial t} - \frac{\partial}{\partial z} \left[ D(\rho_B) \frac{\partial \rho_B}{\partial z} \right] = 0 \quad (14)$$

For polymer-polymer diffusion the diffusion coefficient can be a strong function of composition and can lead to highly unsymmetrical concentration profiles.<sup>14</sup> We appreciate that a completely rigorous analysis of this diffusion couple requires that the partial differential equation in eq 14 be solved with a concentration-dependent diffusion coefficient. For the sake of simplicity, however, we are going to assume that the diffusion coefficient is a constant to see what information can be gleaned from the resulting approximate solution. With this assumption then the species continuity equation becomes

$$\frac{\partial \rho_B}{\partial t} - D \frac{\partial^2 \rho_B}{\partial z^2} = 0 \quad (15)$$

This approximation is commonly called Fick's second law.

The mass density of EMAA[26],  $\rho_B$ , is related to the volume fraction,  $\Phi_B$ , and partial specific volume of EMAA,  $\bar{V}_B$  by

$$\Phi_B = \bar{V}_B \rho_B \quad (16)$$

Assuming that the partial specific volume is constant, the species continuity equation then becomes

$$\frac{\partial \Phi_B}{\partial t} - D \frac{\partial^2 \Phi_B}{\partial z^2} = 0 \quad (17)$$

Equation 17 is valid for systems with constant diffusion coefficients and constant partial specific volumes.

To fully define the diffusion problem, it is now necessary to provide initial and boundary conditions for the second-order partial differential equation given in eq 17. The initial conditions are represented by

$$\Phi_B = 1; \quad z < 0; \quad t = 0 \quad (18)$$

and

$$\Phi_B = 0; \quad z > 0; \quad t = 0 \quad (19)$$

This initial condition states that a step change boundary occurs at  $z = 0$ , the interface between the EMAA[26] and the PVME at  $t = 0$ .

For the boundary conditions we have two choices. The first choice is to assume that the EMAA[26] and PVME regions are infinite in length. This is a good approximation for small times since the materials have had insufficient time to diffuse and they have not come close to the boundaries imposed by the KBr windows. This choice of boundary conditions is represented by

$$\Phi_B = 1; \quad z = -\infty; \quad t > 0 \quad (20)$$

and

$$\Phi_B = 0; \quad z = +\infty; \quad t > 0 \quad (21)$$

The set of equations, initial conditions, and boundary conditions given by eqs 17–21 are satisfied by the standard error function solution:

$$\Phi_B(z,t) = \frac{1}{2} \operatorname{erfc} \left( \frac{z}{2(Dt)^{1/2}} \right) = \frac{1}{2} \left[ 1 - \operatorname{erf} \left( \frac{z}{2(Dt)^{1/2}} \right) \right] \quad (22)$$

Given a value of  $D$ , eq 22 can be used as the solution to the species continuity equation. Thus, the volume fraction of EMAA[26] as a function of time and distance can be determined. In turn,  $\Phi_B(z,t)$  can be employed in conjunction with eqs 3–6 and 12 to determine the fraction of free carbonyl groups,  $f_F(t)$ , as a function of time. Using a nonlinear least-squares regression technique, a best value of  $D$  equal to  $7.7 \times 10^{-16} \text{ cm}^2/\text{s}$  is calculated from a fit to the experimental values of the fraction of free carbonyl groups (Table I). The infinite, open boundary conditions used above are not valid at long times especially near equilibrium since the diffusion of the materials is influenced by the presence of the boundaries imposed by the KBr windows in our experimental technique.

The second choice of boundary conditions is a more accurate, albeit more complex, approximation to reality. At the boundaries imposed by the KBr windows, diffusion is impeded. Therefore, we use the Neumann or "no-flux" boundary conditions represented by

$$\partial \Phi_B / \partial z = 0; \quad z = -L_B; \quad t > 0 \quad (23)$$

and

$$\partial \Phi_B / \partial z = 0; \quad z = +L_A; \quad t > 0 \quad (24)$$

The solution to the diffusion equation, eq 17, in conjunction with the initial conditions, eqs 18 and 19, and the Neumann boundary conditions given by eqs 23 and 24 has been reported by Crank and results in the following:<sup>24</sup>

$$\Phi_B(z,t) = \frac{1}{2} \sum_{n=-\infty}^{+\infty} \left[ \operatorname{erf} \left( \frac{2n(L_A + L_B) - z}{2(Dt)^{1/2}} \right) + \operatorname{erf} \left( \frac{2L_B - 2n(L_A + L_B) + z}{2(Dt)^{1/2}} \right) \right] \quad (25)$$

In a manner similar to that described above for open boundary conditions, eq 25 can be used to obtain a diffusion

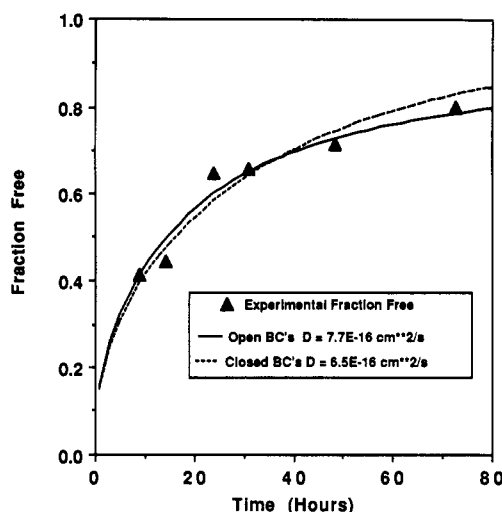


**Figure 5.** Comparison of the experimental fraction of free carbonyl groups as a function of time to the theoretical results for two cases with different boundary conditions.

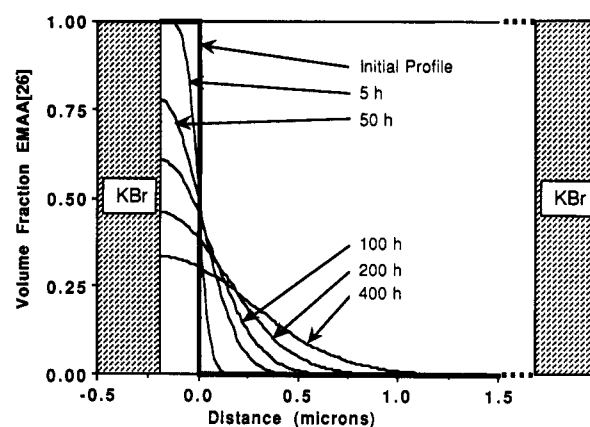
coefficient. This regression to the experimental data results in an estimate of the diffusion coefficient of  $6.5 \times 10^{-16} \text{ cm}^2/\text{s}$ , a result very similar to that obtained for the open boundary conditions. To our knowledge, there have been no prior measurements of mutual diffusion constants reported for polymer-polymer blends involving strong hydrogen bonding. However, the magnitudes of the diffusion constants reported here are certainly within the range of expectation ( $10^{-12}$ – $10^{-16} \text{ cm}^2/\text{s}$ ) for polymer blend systems.<sup>25</sup>

Figure 5 shows a comparison of the experimental fraction of free carbonyl groups to the theoretical curves produced using the above-determined diffusion coefficients. For both open and closed boundary conditions the fit appears to be perfectly reasonable. Perhaps this is not surprising since the diffusion coefficients are regressed from the experimental data. It is important to emphasize that although we obtain a good theoretical fit to the data using a composition-independent diffusion coefficient we cannot conclude that the diffusion coefficient is, or is not, composition dependent. (We are currently developing a numerical procedure to solve the stiff nonlinear partial differential equation with closed boundary conditions in order to investigate the concentration dependence of the diffusion coefficient.)

Figure 6 provides a physical picture of the diffusion process. Concentration profiles for closed boundary conditions were calculated using the value of  $D = 6.5 \times 10^{-16} \text{ cm}^2/\text{s}$ . The initial profile is represented by the sharp, step change in the EMAA[26] volume fraction at the initial interface,  $z = 0$ . It is interesting to note that, even at long diffusion times ( $t = 400 \text{ h}$ ), the system is far removed from equilibrium, which would be represented by a straight, horizontal concentration profile.

## Conclusions

We have presented methods for observing and calculating the mutual diffusion of a miscible polymer blend using transmission FTIR spectroscopy. If we assume that the diffusion coefficient is concentration independent, we obtain a value of  $6.5 \times 10^{-16} \text{ cm}^2/\text{s}$  for the EMAA[26]–PVME couple using closed boundary conditions. Previous diffusion studies by other workers suggest that the



**Figure 6.** Theoretical concentration profiles of EMAA[26] during mutual diffusion with PVME at various times.

diffusion coefficient might be strongly composition dependent, and further experiments are planned similar to those described by Jones et al.,<sup>10</sup> using the transmission infrared method described here, to see if it is feasible to determine composition-dependent diffusion coefficients.

**Acknowledgment.** We gratefully acknowledge the financial support of the National Science Foundation, Polymers Program, and the E. I. du Pont de Nemours Co. Conversations with Professor J. L. Duda and Dr. J. Harrell are gratefully acknowledged.

## References and Notes

- (1) Bueche, F. J. *Chem. Phys.* **1952**, *20*, 1959.
- (2) Bueche, F. J. *Chem. Phys.* **1956**, *25*, 599.
- (3) Bueche, F. J. *Chem. Phys.* **1968**, *48*, 1410.
- (4) Tanner, J. E. *J. Chem. Phys.* **1970**, *52*, 2523.
- (5) von Meerwall, E. D. *Adv. Polym. Sci.* **1984**, *54*, 1.
- (6) Bachus, R.; Kimmich, R. *Polymer* **1983**, *24*, 964.
- (7) Tead, S. F.; Kramer, E. J. *Macromolecules* **1988**, *21*, 1513.
- (8) Kumagai, Y.; Watanabe, H.; Miyasaka, K.; Hata, T. *J. Chem. Eng. Jpn.* **1979**, *12*, 1.
- (9) Composto, R. J.; Kramer, E. J.; White, D. M. *Nature* **1987**, *328*, 234.
- (10) Jones, R. A. L.; Klein, J.; Donald, A. M. *Nature* **1986**, *321*, 161.
- (11) Price, F. P.; Gilmore, P. T.; Thomas, E. L.; Laurence, R. L. *J. Polym. Sci., Polym. Symp.* **1978**, *63*, 33.
- (12) Gilmore, P. T.; Falabella, R.; Laurence, R. L. *Macromolecules* **1980**, *13*, 880.
- (13) Garbella, R. W.; Wendorff, J. K. *Makromol. Chem., Rapid Commun.* **1986**, *7*, 591.
- (14) Klein, J. *Nature* **1978**, *271*, 143; *Science* **1990**, *250*, 640.
- (15) Klein, J.; Briscoe, B. J. *Proc. R. Soc. London A* **1979**, *365*, 53.
- (16) Klein, J.; Fletcher, D.; Fetters, L. J. *Nature* **1983**, *304*, 526.
- (17) Jordon, E. A.; Ball, R. C.; Donald, A. M.; Fetters, L. J.; Jones, R. A. L.; Klein, J. *Macromolecules* **1988**, *21*, 235.
- (18) Coleman, M. M.; Graf, J. F.; Painter, P. C. *Specific Interactions and the Miscibility of Polymer Blends*; Technomic Publishing Co., Inc.: New Holland, PA, 1991.
- (19) Lee, J. Y.; Painter, P. C.; Coleman, M. M. *Macromolecules* **1988**, *21*, 346.
- (20) Coleman, M. M.; Lee, J. Y.; Serman, C. J.; Wang, Z.; Painter, P. C. *Polymer* **1989**, *30*, 1298.
- (21) Lee, J. Y.; Painter, P. C.; Coleman, M. M. *Macromolecules* **1988**, *21*, 954.
- (22) Lichkus, A. M.; Painter, P. C.; Coleman, M. M. *Macromolecules* **1988**, *21*, 2636.
- (23) Duda, J. L.; Vrentas, J. S. *Ind. Eng. Chem. Fund.* **1965**, *4*, 301.
- (24) Crank, J. *Mathematics of Diffusion*; Oxford University Press: London, U.K., 1975.
- (25) Composto, R. J.; Kramer, E. J.; White, D. M. *Macromolecules* **1988**, *21*, 2580.

**Registry No.** EMAA (copolymer), 25053-53-6; PVME (homopolymer), 9003-09-2.